

UDK: 666.112.3; 624.044; 620.181.4

The Thermophysical Properties of Primary Phase in Lithium Germanium Phosphate Glass

Srdjan D. Matijašević^{1*)}, Vladimir S. Topalović¹, Snežana R. Grujić²,
Veljko V. Savić¹, Jelena D. Nikolić¹, Nebojša J. Labus³, Snežana N.
Zildžović¹

¹Institute for Technology of Nuclear and Other Mineral Raw Materials (ITNMS),
Franchet d Esperey 86, 11000 Belgrade, Serbia

²Faculty of Technology and Metallurgy, University of Belgrade, Karnegijeva 4, 11000
Belgrade, Serbia

³Institute of Technical Sciences of SASA, Knez Mihailova 35/IV, 11000 Belgrade,
Serbia

Abstract:

The selected lithium germanium-phosphate glass was prepared by a conventional melt-quenching technique. The XRD method was employed to confirm the glass was obtained and to reveal crystalline phases during heat treatment. The dilatometry (DIL), differential thermal analysis (DTA), and differential scanning calorimetry (DSC) were used to determine the characteristic temperatures and enthalpies of crystallization and melting of the crystalline phase. The DTA and DIL were used to obtain the viscosity curves by applying the Vogel-Fulcher-Tammann (VFT) equation.

Keywords: Lithium germanium-phosphate glass; DTA; Dilatation; DSC.

1. Introduction

Glass is a unique state of matter that combines features of both liquids and solids and also exhibits its unique characteristics [1]. It is nonequilibrium, noncrystalline condensed state of matter that exhibits a glass transition [2]. The characteristics of this unique material are determined not only by its chemical and physical properties but also by its thermal history and properties (heating and cooling rate, characteristic temperatures T_g , T_x , T_c , T_m) [3]. For the characterization of glasses and obtaining glass-ceramics, it is mandatory to determine characteristic temperatures and viscosity. Lithium germanium phosphate glasses have recently emerged as multipurpose materials and have been given great attention because of their potential applications in various solid-state devices [4]. The synthesis of the parent glass is an important step in preparing the final glass-ceramic material because the precursors and their percentage in the glass composition manage the precipitation of the crystalline phases [5]. By crystallization of some glasses from the system $\text{Li}_2\text{O}-\text{Al}_2\text{O}_3-\text{GeO}_2-\text{P}_2\text{O}_5$, the $\text{LiGe}_2(\text{PO}_4)_3$ phase which belongs to the solid solutions with the general formula of $\text{Li}_{1+x}\text{M}_x\text{Ge}_{2-x}(\text{PO}_4)_3$ ($\text{M}=\text{Al}$, V or Cr) is formed. The role of Al^{3+} ions in glass matrix (similarity in ionic radius between Ge^{4+} (0.053 nm) and Al^{3+} (0.050 nm) was to improve the porous density of $\text{LiGe}_2(\text{PO}_4)_3$ phase and also to introduces additional vacant lattice sites, which enhances the Li-ion diffusion and consequently leads to higher ionic conductivity with lower activation

*) Corresponding author: s.matijasevic@itnms.ac.rs

energy [6]. This family of crystalline phosphates is often referred to as NASICON-type materials [7]. They exhibit distinctive ionic conductivities of 10^{-4} – 10^{-3} S/cm at room temperature [8, 9]. In this study, $\text{LiGe}_2(\text{PO}_4)_3$ has been synthesized and its thermo-physical properties were investigated. The tested compound is a candidate as anode material for Li-ion batteries because of the low potential of the $\text{Ge}^{4+}/\text{Ge}^{3+}$ redox couple versus Li/Li^+ . For this investigation, the glass composition $22.5\text{Li}_2\text{O}\cdot 10\text{Al}_2\text{O}_3\cdot 30\text{GeO}_2\cdot 37.5\text{P}_2\text{O}_5$ (mol%) was selected.

2. Materials and Methods

The glass was prepared by melting a homogeneous mixture of reagent-grade Li_2CO_3 (Fluka p.a), Al_2O_3 (Fluka p.a.), GeO_2 (Acros pur.spec.), and $(\text{NH}_4)_2\text{HPO}_4$ (Fluka p.a) in a covered platinum crucible. The melting was performed in an electric furnace BLF 17/3 at $T=1400$ °C during $t=0.5$ h. The melt was then quenched on a steel plate at room temperature and pressed with another steel plate immediately to form a thin glass disc.

2.1. Chemical analysis

The chemical analysis was performed using spectrophotometer AAS PERKIN ELMER Analyst 703. The method of atomic absorption spectrophotometry (AAS) was used to determine the content of oxides, Li_2O , GeO_2 , P_2O_5 , Al_2O_3 in glass, after the destruction of the sample by NaOH, the composition was determined by analyzing the content of their cations in the solution. The measurement uncertainty is 0.86 %.

2.2. Density

The density of the synthesized sample was determined using Archimedes principle by the pycnometer method with a measurement accuracy of ± 0.90 % [10]. The experimental error was estimated after 3 parallel measurements. All the measurements have been recorded at room temperature ($T=20$ °C).

2.3. X-ray diffraction analysis (XRD)

Identification of crystalline phases formed during heat treatment of glass samples at crystallization peak temperatures was performed by X-ray analysis. The PHILIPS PW 1710 automatic diffractometer with the following characteristics was used for measurement: - X-ray tube Cu LFF 40 kW; 32 mA; - graphite monochromator and proportional counter with xenon; - recording area (2θ) from 4 to 70° (- scan time from 0 to 5 s) with 0.02° step size. The intensities of diffracted $\text{CuK}\alpha_1$ X-rays ($\lambda = 0.154060$ nm) were measured at room temperature.

2.4. Differential-thermal analysis (DTA)

The behavior of the glass during heating was monitored using DTA, on a DTA / TGA device NETZSCH STA 409EP under the following conditions: particle size of glass powder (0.5-0.65 mm), sample weight 100 mg, temperature measuring range from $T = 20$ - 1100 °C, sample heating rate $\beta = 10$ °C /min, Al_2O_3 was used as a reference substance in a static air atmosphere. Glass powder for analysis was prepared by crushing and grinding bulk glass in an agate mortar and sieving on a standard series of sieves. Before the DTA experiment, the device was calibrated with quartz standard purity of 99.995 % of known crystallization

temperature. The characteristic temperatures of the tested glasses determined from the DTA curve, were transformation temperature (T_g), crystallization temperature range (exothermic peak temperature T_c), and melting point temperature (liquidus) (T_m).

2.5. Dilatometric analysis (DIL)

The standard dilatometric method ISO 7884-8 was used to determine the glass transformation temperature (T_g) and the dilatometric softening temperature (T_d) [11]. Measurements were performed on a dilatometer Baehr Geratebau GmbH D802, in an air atmosphere with a displacement resolution of 20 nm and temperature resolution of 1 °C. Due to the low viscosity of the melt, the technique of pouring the melt on a steel plate placed at an angle to obtain samples for dilatometric measurements was used. The bulk samples were then annealed in an electric furnace CARBOLITE CWF 13/13 in a given temperature regime (Table I) to remove the thermal stresses:

Tab. I Temperature regime of glass annealing.

T [°C]	β [°C/min]*	β_c [°C/min]*
20-540	10	-
540-300	-	1.0
300-20	-	air cooling in the furnace

* β -heating rate, β_c -cooling rate

A diamond saw was used to cut the rods of suitable dimensions from the sample thus obtained ($l = 50$ mm; $d = 3-5$ mm) and to process the surface sides and edges.

Sample preparation is important for accurate dilatometry since the samples must be well consolidated and cut with two plan parallel side planes at a known distance.

2.6. Differential scanning calorimetry (DSC)

The enthalpy of crystallization ΔH_c and the enthalpy of melting of the crystalline phase ΔH_m were determined using differential scanning calorimetry (DSC). For this experiment, a sample of glass with granulation of 0.50-0.65 mm at a heating rate $\beta = 20$ °C/min on the device TA Instruments SDT Q600 V7.0 BUILD 84 was used. The curve was recorded up to $T = 1130$ °C, with a sample weight of 10 mg. Before the DSC experiment, the device was calibrated with silver and zinc standards purity of 99.999 % of known melting enthalpies.

3. Results and Discussion

The glass mixture for obtaining the selected glass composition was melted in an electric furnace. The resulting melts were poured between two steel plates and cooled in the air. During cooling, the melt solidified into a transparent, homogeneous, and colorless glass. The XRD analysis confirmed the quenched melts to be vitreous (figure not shown). The results of the chemical analysis show that a glass composition of $22.5\text{Li}_2\text{O} \cdot 10\text{Al}_2\text{O}_3 \cdot 30\text{GeO}_2 \cdot 37.5\text{P}_2\text{O}_5$ (mol%) (LAGP) was obtained.

The density of obtained glass is $\rho = (3.34 \pm 0.04)$ g/cm³ determined by the standard pycnometer method. To identify the formed crystal phases, the bulk samples were crystallized in one-stage heat treatment at $T = 800$ °C for $t = 100$ h. The XRPD analysis confirmed the primary crystallization of selected glass.

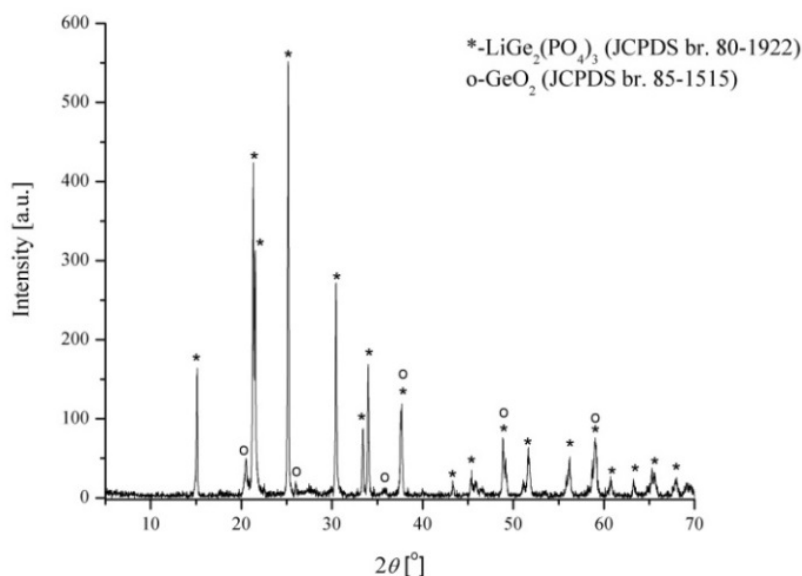


Fig. 1. XRD analysis of LAGP glass sample crystallized at $T = 800\text{ }^{\circ}\text{C}$ for $t = 100\text{ h}$

From Fig. 1, it can be noticed the high content of the required $\text{LiGe}_2(\text{PO}_4)_3$ crystalline phase as the primary and the presence of GeO_2 as the secondary phase. Crystalline phases separated during heat treatment were identified using JCPDS cards [12]. The density of obtained primary crystalline phase is $\rho = (3.60 \pm 0.05)\text{ g/cm}^3$ determined by the standard pycnometer method.

The molar volume $V_m = (121.43 \pm 0.05) \cdot 10^{-6}\text{ m}^3/\text{mol}$ of the $\text{LiGe}_2(\text{PO}_4)_3$ crystalline phase was calculated using the relative molecular mass ($M = 437.14\text{ g/mol}$) and density (ρ) by the following relation [13]:

$$V_m = m/\rho \quad (1)$$

The porosity of the $\text{LiGe}_2(\text{PO}_4)_3$ phase was found to be as high as 26 %, reported by earlier investigation [14].

DTA provides an overview of the transformations that the glasses undergo at different temperatures, such as the glass transition T_g (manifested by the first inflection in the trace), onset crystallization temperature T_x , crystallization temperature T_c (characterized by exothermic peak), and melting temperature T_m (characterized by endothermic peak). This section presents the results of the glass powders crystallization test on DTA under nonisothermal conditions. The DTA curve of the LAGP glass powder composition with 0.50-0.65 mm granulation was heated at a constant heating rate $\beta = 10\text{ }^{\circ}\text{C/min}$ up to $1100\text{ }^{\circ}\text{C}$ is shown in Fig. 2.

The DTA curve from Fig. 2, shows a bend corresponding to the glass transformation temperature $T_g = 516\text{ }^{\circ}\text{C}$, exothermic peaks in the region $640\text{--}740\text{ }^{\circ}\text{C}$ with a maximum at $T_{c1} = 665\text{ }^{\circ}\text{C}$ which indicates glass crystallization and a wider endothermic peak in the region $1030\text{--}1090\text{ }^{\circ}\text{C}$ which represents the melting of the present crystalline phase in the glass with a minimum at $T_m = 1074\text{ }^{\circ}\text{C}$. A smaller exothermic peak at $736\text{ }^{\circ}\text{C}$ indicates the presence of another phase in a very small amount. Considering the previously presented XRD pattern of the crystallized glass sample, the peak at $T_{c1} = 665\text{ }^{\circ}\text{C}$ is attributed to the crystallization of primary $\text{LiGe}_2(\text{PO}_4)_3$ phase, NASICON type crystal precipitated in glass matrix (rhombohedral crystal system, space group R3c), while the peak at $T_{c2} = 736\text{ }^{\circ}\text{C}$ is connected with the crystallization of secondary $\alpha\text{-GeO}_2$ phase appeared in traces (2.4 vol%) [15]. Also, according to the temperature difference between $(T_x - T_g) > 125\text{ }^{\circ}\text{C}$, the process of sintering can

be independent of crystallization, and LAGP glass can be suitable for engineering and manufacturing [16-18]. Also, this glass has volume crystallization [16, 19].

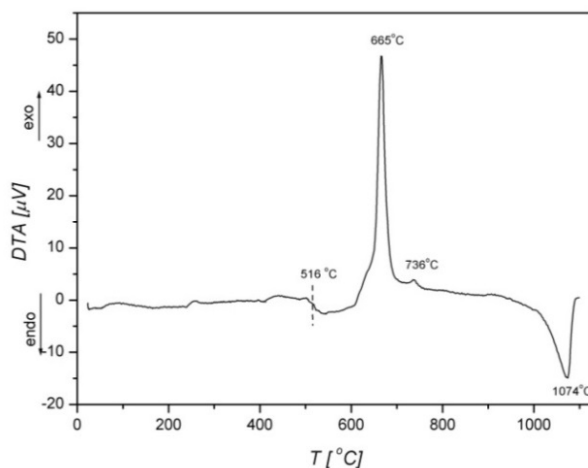


Fig. 2. DTA curve of LAGP powder, sample granulation 0.5-0.65 mm, $m_g = 100$ mg, $\beta = 10$ $^{\circ}$ C/min, shows thermal peaks.

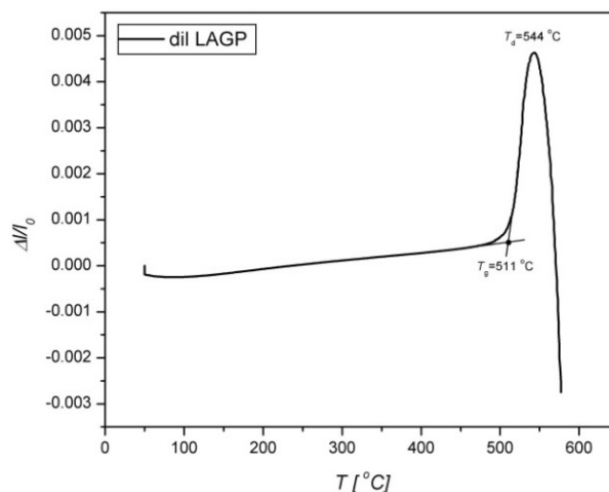


Fig. 3. The dilatometric curve of LAGP glass.

The thermal expansion curve measured by dilatometry gives three important properties – the thermal expansion coefficient (α), glass transformation temperature (T_g), and dilatometric softening temperature (T_d). By increasing the temperature, the specimen's size enlarges because the volume of glass increases. The dilatometric curve of the LAGP glass sample heated to $T = 600$ $^{\circ}$ C, at the speed $\beta = 5$ $^{\circ}$ C/min is shown in Fig. 3. The sudden expansion in the temperature range 510-540 $^{\circ}$ C is referred to as the transformation range and indicates the onset of viscoelastic behavior, where bond breaking in the glass is predominant. The glass phase transformation temperature with an onset temperature of transformation, at $T_g = 511$ $^{\circ}$ C and the dilatometric softening temperature $T_d = 544$ $^{\circ}$ C, as the temperature of maximum expansion, were determined on the curve, Fig. 3. Softening point corresponds to the viscous flow of the sample under stresses imposed by the dilatometric push rod.

After the dilatometric softening temperature, a sharp sample shrinkage occurs at temperatures higher than $T = 560$ $^{\circ}$ C. The experiment had to be stopped because further heating could lead to the fusing of the melted sample with the measuring cell. The cooling of the glass sample enables extraction in its bulk form [20].

Based on the analysis, the determined dilatometric transformation temperature T_g corresponds to the value determined from the DTA curve, taking into account the experimental error during the determination.

DSC is the most common thermal analysis technique used for a wide range of applications, including fundamental research, development of new materials, and an especially important characterization technique in the field of glass science and technology [21, 22]. The DSC curve of a glass sample of LAGP composition with granulation of 0.5-0.65 mm is shown in Fig. 4.

The characteristic temperatures, as well as both enthalpies of crystallization and melting of the existing phase, were determined on the curve, while the corresponding molar enthalpies were calculated. The measured temperatures of crystallization ($T_c = 681.7^\circ\text{C}$) and melting ($T_m = 1095.5^\circ\text{C}$) are slightly higher than on the DTA curve due to the higher heating rate during recording. It should be emphasized that the heating rate of the sample does not affect the determination of the molar enthalpies of crystallization and melting of the crystalline phase.

The enthalpy of crystallization (for the exothermic maximum in Fig. 4) of 110.7 J/g and the enthalpy of melting of the crystalline phase (endothermic maximum in Fig. 4) of 138 J/g were determined.

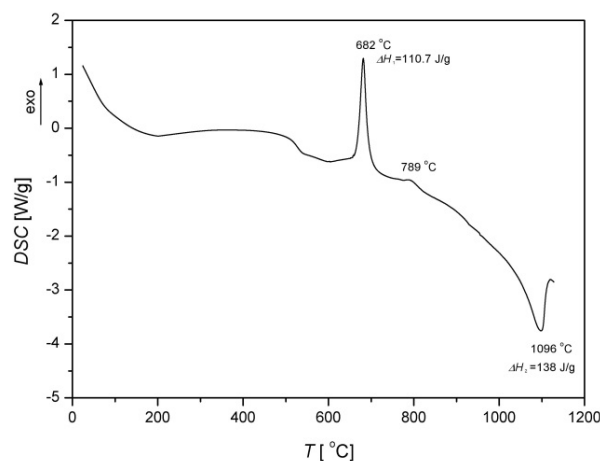


Fig. 4. DSC diagram of LAGP glass composition.

Thermodynamic data for the crystalline phase of $\text{LiGe}_2[\text{PO}_4]_3$ were determined based on the DSC diagram (Fig. 4). The molar enthalpy of crystallization is $\Delta H_c = 48.391 \text{ kJ/mol}$ for the exothermic peak (110.7 J/g), and the molar enthalpy of melting $\Delta H_m = 60.325 \text{ kJ/mol}$ for the endothermic peak (138.0 J/g). The change in heat capacity during the transformation of the subcooled melt and $\text{LiGe}_2[\text{PO}_4]_3$ phase crystals was determined using the equation:

$$\Delta C_p = (\Delta H_m - \Delta H_c) / (T_m - T_c) \quad (2)$$

The calculated value of the change in heat capacity is $\Delta C_p = 28.84 \text{ J/(mol}\cdot\text{K)}$. The required calculation parameters were read and calculated from the DSC diagram. The melting entropy of the tested glass is $\Delta S_m = 44.08 \text{ J/(mol}\cdot\text{K)}$ and it is calculated from the molar enthalpy of melting (ΔH_m). The change in free energy of the liquid / solid phase transformation (ΔG) from the undercooled melt as a function of temperature was determined using equation (3):

$$\Delta G = -\frac{\Delta H_m}{T_m}(T_m - T) + \Delta C'_p \left[(T_m - T) - T \ln\left(\frac{T_m}{T}\right) \right] \quad (3)$$

$$\Delta G(T) = -44.08 \cdot (1368.65 - T) + 28.84 \left[(1368.65 - T) - T \ln(1368.65/T) \right], \text{ [J/mol]}$$

where the temperature (T) is given in Kelvins [K].

The viscosity dependence on temperature of tested glass was determined using the Vogel - Fulcher - Tammann (VFT) equation in the form [23]:

$$\log \eta = A + B/(T - T_0) \quad (4)$$

where A , B , and T_0 are the empirical parameters calculated from three experimentally determined temperatures - T_g (transformation temperature), T_d (softening temperature), and T_m (melting temperature) which correspond to the viscosity reference values ($\log \eta$). Characteristic temperatures were determined by DTA and the dilatometric method (Fig. 2 and 3). The data used to calculate the constants are shown in Table II.

Tab. II Data for calculating A , B and T_0 parameters.

Determination methods	Dilatation	Dilatation	DTA
Characteristic temperatures	T_g	T_d	T_m
T [°C]	511	544	1074
$\log \eta$	12.2	10.3	1.5

The VFT equation describing the viscosity of the test glass was obtained in the form:

$$\log \eta = -2.8361 + 3430.6 / (T - 555.8459) \quad (5)$$

where the corresponding units are given in the SI system: viscosity (η) is given in [Pa · s], and temperature (T) in Kelvins [K]. The corresponding viscosity curve of the LAGP glass composition as a function of temperature is given in Fig. 5.

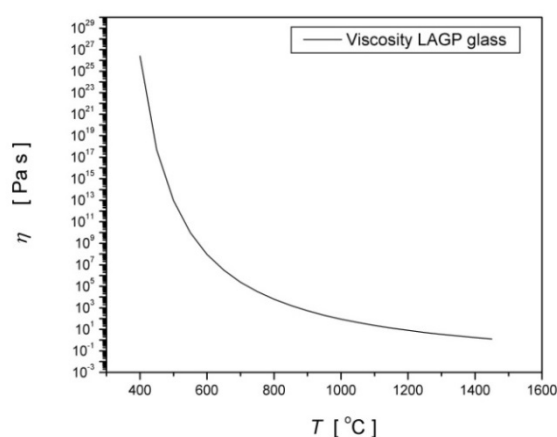


Fig. 5. Dependence η - T for the tested LAGP glass.

By knowing the viscosity of glass, it is possible to determine when the glass is in solid form, when it is in the melting phase, and when it is in the transformation region (the temperature region between the cooled melt and the solid phase in the unbalanced state is called the transition region or glass transformation region). Also, based on viscosity, the area of glass processing can be determined. One of the most important factors in the production of glass articles is the variation of glass viscosity under changing temperature. All glasses can be arbitrarily classified as “short,” i.e., fast-solidifying glasses, and “long” ones that solidify slowly.

It is generally accepted that the limiting values of viscosity in making glass articles are 10^2 - 10^8 Pa·s. Therefore, the temperature interval of glass manufacture is restricted by the specified viscosity values and lies within a range from a few tens to a few hundred degrees. According to the temperature interval of 370 °C for glass viscosity 10^2 - 10^8 Pa·s this glass belongs to long therm glasses, Fig. 5 [24].

Based on the gathered temperature dependence of the viscosity, the activation energy of the viscous flow $E_\eta = \Delta G_\eta$ [25] was obtained from the Arrhenius equation and calculated from the slope of the line $\log(\eta) = f(1/T)$, which is shown in Fig. 6.

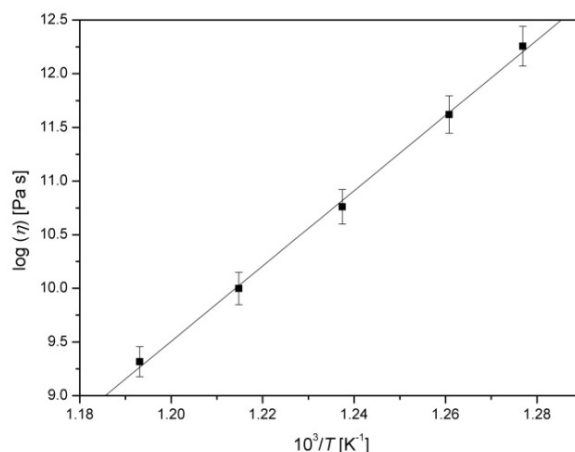


Fig. 6. $\log(\eta)$ versus $(1/T)$ for LAGP glass.

The activation energy of the viscous flow in the temperature range 500-570 °C is $\Delta G_\eta = (671 \pm 16)$ kJ / mol.

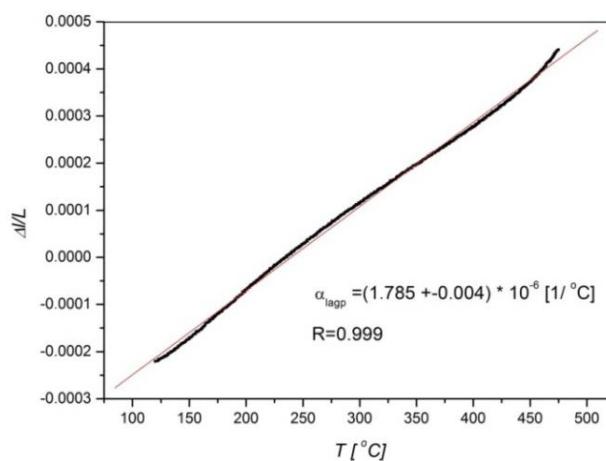


Fig. 7. Determination of the coefficient of linear thermal expansion of LAGP glass.

For glasses, the measured expansion coefficient is one-directional and the measured value is linear thermal expansion coefficient (α_l). The linear thermal expansion coefficient value of commercial glasses is measured over a specified temperature range and in most cases from 0-300 °C [26].

Based on the dilatometric analysis, the coefficient of linear thermal expansion of glass was determined, which is $\alpha_{lagp} = (1.79 \pm 0.01) \cdot 10^{-6}$ 1/°C in the temperature range of 100-500 °C (Fig. 7). The coefficient of linear thermal expansion of $\text{LiGe}_2[\text{PO}_4]_3$ ceramic phase was reported earlier as $7.0 \cdot 10^{-6}$ 1/°C within a temperature range of 20-1000 °C, as near-zero expansion ceramics [27]. This property (linear thermal expansion coefficient) is utilized in

tempering processes for generating compressive surface layers to prevent flaw propagation, hence increasing strength [28].

NASICON type materials (as obtained LAGP glass or ceramic) show low thermal expansion behavior, which was exploited in some of the applications (thermal shock, high-energy lasers, precision optics, household ovenware, and giant telescope mirrors) of these materials [29, 30].

4. Conclusion

The parent glass from the system $22.5\text{Li}_2\text{O}\cdot 10\text{Al}_2\text{O}_3\cdot 30\text{GeO}_2\cdot 37.5\text{P}_2\text{O}_5$ (mol%) was prepared by standard melt-quenching technique.

The characteristic temperatures, density, molar volume, thermal expansion coefficient, and viscosity of the obtained glass were determined from experimental analyses. The change in free energy of the liquid / solid phase transformation from the undercooled melt as a function of temperature, as well as the activation energy of the viscous flow, were determined. Obtained LAGP glass, shows low thermal expansion behavior, and in the field of glass, processing solidifies slowly (between limiting values of viscosity in making glass particles). Based on the thermal properties obtained glass is suitable for engineering and manufacturing. The study of the LAGP glass crystallization process revealed the NASICON $\text{LiGe}_2(\text{PO}_4)_3$ phase. The exploration of NASICON materials could provide new electrode materials for lithium-ion batteries.

Acknowledgments

The authors are grateful to the Ministry of Education, Science and Technological Development of the Republic of Serbia for the financial support (grant contract No.: 451-03-9/2021-14/200023).

5. References

1. Q. Zheng, Y. Zhang, M. Montazerian, O. Gulbiten, J. C. Mauro, E. D. Zanotto, Y. Yue, *Chem. Rev.*, 119 (2019) 7848-7939.
2. E. D. Zanotto, J. C. Mauro, *J. Non-Cryst. Solids*, 471 (2017) 490-495.
3. J. N. Stojanović, S. V. Smiljanić, S. R. Grujić, P. J. Vulić, S. D. Matijašević, J. D. Nikolić, V. V. Savić, *Sci. Sinter.*, 51 (4) (2019) 389-399.
4. C. Masquelier, *Nat. Mater.*, 10 (2011) 649-650.
5. J. Maletaškić, B. Todorović, M. Gilić, M. Marinović-Cincović, K. Yoshida, A. Gubarevich, B. Matović, *Sci. Sinter.*, 52 (1) (2020) 41-52.
6. M. M. Mahmoud, Y. Cui, M. Rohde, C. Ziebert, G. Link, H. J. Seifert, *Materials*, 9 (2016) 506-519.
7. N. Anantharamulu, K. K. Rao, G. Rambabu, B. V. Kumar, V. Radha, M. Vithal, *J. Mater. Sci.*, 46 (2011) 2821-2837.
8. R. DeWees, H. Wang, *Chem. Sus. Chem.*, 12 (16) (2019) 3713-3725.
9. A. Dapčević, A. Radojković, M. Žunić, M. Počuća-Nešić, O. Milošević, G. Branković, *Sci. Sinter.*, 53 (1) (2021) 55-66.
10. S. H. Jaafar, M. H. M. Zaid, K. A. Matori, M. S. M. Ghazali, M. F. S. M. Shofri, N. A. N. Hisham, D. I. Saparudin, *Sci. Sinter.*, 52 (3) (2020) 269-281.
11. International standard ISO 7884-8E (1987)
12. Powder Diffraction File, Joint Committee on Powder Diffraction Standards, Centre for Diffraction Data, Swarthmore, PA (1988)

13. S. V. Smiljanić, S. R. Grujić, M. B. Tošić, V. D. Živanović, S. D. Matijašević, J.D. Nikolić, V. S. Topalović, Chem. Ind. Chem. Eng. Q., 22 (1) (2016) 111-115.
14. C. J. Leo, G. V. Subba Rao, B. V. R. Chowdari, Solid State Ion., 159 (2003) 357-367.
15. J. D. Nikolić, S. V. Smiljanjić, S. D. Matijašević, V. D. Živanović, M. B. Tošić, S. R. Grujić, J. N. Stojanović, Process. Appl. Ceram., 7 (4) (2013) 147-151.
16. S. D. Matijašević, S. R. Grujić, V. S. Topalović, J. D. Nikolić, S. V. Smiljanić, N. J. Labus, V.V. Savić, , Sci. Sinter., 50 (2) (2018) 193-203.
17. M. Kamyabi, R. Sotudeh-Gharebagh, R. Zarghami, K. Saleh, Chem. Eng. Res. Des., 125 (2017) 328-347.
18. V. S. Topalović, S. R. Grujić, V. D. Živanović, S. D. Matijašević, J. D. Nikolić, J. N. Stojanović, S. V. Smiljanić, Ceram. Int., 43 (15) (2017) 12061-12069.
19. E. D. Zanotto, V. M. Fokin, Phil. Trans. R. Soc. Lond. A 361 (2003) 591-613.
20. J. D. Musgraves, J. Hu, L. Calvez, Springer Handbook of Glass, Springer International Publishing AG Switzerland, 2019.
21. M. Montazerian, S. P. Singh, E. D. Zanotto, Am. Ceram. Soc. Bull., 94 (2015) 30-35.
22. Q. Zheng,, Y. Zhang, M. Montazerian, O. Gulbitten, J. C. Mauro, E. D. Zanotto, Y.Yue, Chem.Rev., 119 (2019) 7848-7939.
23. C. Guillemet, R. Gy, Rev. Metall., 93 (5) (1996) 701-710.
24. V. S. Bessmertnyi, V. P. Krokhin, V. Panasenko, N. Drizhd, P. Dyumina, O. Kolchina, Glass Ceram., 58 (2001) 176-179.
25. J. Hlavač, The Technology of Glass and Ceramics, Elsevier Sci.Pub.Comp., New York, 1983.
26. J. E. Shelby, Introduction to Glass Science and Technology, 2nd edition, The Royal Society of Chemistry, Cambridge, UK, 2005.
27. V. I. Petkov, A. I. Orlova, Inorg. Mater., 39 (10) (2003) 1013-1023.
28. M. Hasanuzzaman, A.Rafferty, M.Sajjia, A.-G.Olabi, Properties of Glass Materials, Chapter in Reference Module in Materials Science and Materials Engineering, Elsevier, Amsterdam, Netherlands, 2016.
29. R. Roy, D. K. Agrawal, J. Alamo, R.A. Roy, Mater. Res. Bull. 19 (1984) 471-477.
30. V. I. Petkov, A. I. Orlova, Inorganic Materials, 39 (10) (2003) 1013-1023.

Сажетак: Одабрано литијум-германијум-фосфатно стакло припремљено је конвенционалном техником топљењем. ХРД метода је коришћена за потврду добијене аморфне структуре и анализу кристалних фаза током топлотне обраде. Дилатометрија (ДИЛ), диференцијална термичка анализа (ДТА) и диференцијална скенирајућа калориметрија (ДСК) коришћене су за одређивање карактеристичних температура и енталпија кристализације и топљења кристалне фазе. ДТА и ДИЛ су коришћени за добијање криве вискозности применом једначине Vogel-Fulcher-Tammann (ВФТ).

Кључне речи: Литијум-германијум-фосфатно стакло, ДТА, Дилатација, ДСК.

© 2021 Authors. Published by association for ETRAN Society. This article is an open access article distributed under the terms and conditions of the Creative Commons — Attribution 4.0 International license (<https://creativecommons.org/licenses/by/4.0/>).

